Activation by Cdc42 and PIP_2 of Wiskott-Aldrich Syndrome protein (WASp) Stimulates Actin Nucleation by Arp2/3 Complex

Henry N. Higgs and Thomas D. Pollard

The Salk Institute for Biological Studies, La Jolla, California 92037

Abstract. We purified native WASp (Wiskott-Aldrich Syndrome protein) from bovine thymus and studied its ability to stimulate actin nucleation by Arp2/3 complex. WASp alone is inactive in the presence or absence of 0.5 μM GTP-Cdc42. Phosphatidylinositol 4,5 bisphosphate (PIP_2) micelles allowed WASp to activate actin nucleation by Arp2/3 complex, and this was further enhanced twofold by GTP-Cdc42. Filaments nucleated by Arp2/3 complex and WASp in the presence of PIP_2 and Cdc42 concentrated around lipid micelles and vesicles, providing that Cdc42 was GTP-bound and prenylated. Thus, the high concentration of WASp in neutrophils (9 μM) is dependent on interactions with both acidic lipids and GTP-Cdc42 to activate actin nucleation by Arp2/3 complex. The results also suggest that membrane binding increases the local concentrations of Cdc42 and WASp, favoring their interaction.

Key words: prenylation • membrane • GBD • neutrophil • thymus

Introduction

Arp2/3 complex (Machesky et al., 1994) initiates the barbed end growth of actin filaments by enhancing their nucleation (Mullins et al., 1998). Filaments initiated by Arp2/3 complex grow from the sides of other actin filaments to form branches in a process termed dendritic nucleation. Dendritic nucleation occurs at the leading edge of motile cells, and Arp2/3 complex localizes to branch points (Bailly et al., 1999; Svitkina and Borisy, 1999). The importance of Arp2/3 complex for actin dynamics in general is supported by work in diverse organisms including the following: mammalian tissue culture cells (Machesky et al., 1997; Welch et al., 1997a; Machesky and Insall, 1998) and lymphocytes (Weiner et al., 1999); extracts from brain (Ma et al., 1998b) and *Acanthamoeba* (Mullins and Pollard, 1999); and genetics in both budding (Winter et al., 1999b) and fission yeast (Balasubramanian et al., 1996; McCollum et al., 1996; Morrell et al., 1999).

Highly purified Arp2/3 complex alone does not enhance actin nucleation unless activated by members of the WASp/Scar protein family (Higgs et al., 1999; Machesky et al., 1999; Rohatgi et al., 1999; Winter et al., 1999a; Yarar et al., 1999) or bacterial proteins (Welch et al., 1998). Activation by WASp/Scar proteins requires only their COOH-terminal 70–100 amino acids, termed the WA region (see Fig. 1 A). WA contains an actin-binding WH2 motif, an Arp2/3 complex–binding COOH-terminal acidic motif, and a connecting region in between, which might contribute to activation (Marchand et al., 2000).

Mammals have genes for at least five WASp/Scar proteins (for review see Higgs and Pollard, 1999). Wiskott-Aldrich Syndrome protein (WASp)[1] appears to be restricted to hematopoietic cells and mutations to the WASp gene can cause Wiskott-Aldrich Syndrome, causing defects in platelets and lymphocytes (Ochs, 1998). N-WASP is closely related in sequence to WASp and is more widely expressed (Miki et al., 1996). Less is known about the three Scar isoforms, also called WAVE (Suetsugu et al., 1999).

WA regions of WASp/Scar proteins constitutively activate Arp2/3 complex. The NH_2-terminal 85% of these proteins contain sequences capable of interacting with many other proteins including the following: the Rho family GTPase, Cdc42; Src family tyrosine kinases; Tec family tyrosine kinases; the adaptor proteins, Nck and Grb2; and calmodulin (for review see Higgs and Pollard, 1999). An attractive model for WASp regulation (Miki et al., 1998; Kim et al., 2000) is that the NH_2-terminal region autoinhibits the COOH-terminal WA region, and binding of regulatory

Address correspondence to Thomas D. Pollard, The Salk Institute for Biological Studies, 10010 North Torrey Pines Road, La Jolla, CA 92037. Tel.: (858) 453-4100 x1716. Fax: (858) 452-3683. E-mail: pollard@salk.edu

[1]*Abbreviations used in this paper:* CF-PE, carboxyfluorescein-labeled PE; GBD, GTPase binding domain; GST, glutathione-S-transferase; HSS, high speed supernatant; PA, phosphatidic acid; PC, phosphatidylcholine; PE, phosphatidylethanolamine; PIP_2, phosphatidylinositol 4,5 bisphosphate; PS, phosphatidylserine; PMN, polymorphonuclear leukocytes; WA, WASp/Scar protein COOH-terminal 70–100 amino acids; WASp, Wiskott-Aldrich Syndrome protein.

proteins to NH_2-terminal sequences relieves this inhibition, resulting in Arp2/3 complex activation and actin nucleation. The lipid second messenger, phosphatidylinositol-4,5-bisphosphate (PIP_2), also might bind WASp and N-WASP and might assist in activation (Rohatgi et al., 1999).

Several lines of evidence support the model that GTP-bound Cdc42 (GTP-Cdc42) activates WASp or N-WASP by relief of autoinhibition. GTP-Cdc42 strongly stimulates actin nucleation in resting cell extracts (Zigmond et al., 1997; Ma et al., 1998a; Mullins and Pollard, 1999). Nuclear magnetic resonance structures show that GTP-Cdc42 binds a specific region (GTPase binding domain or GBD) on WASp and N-WASP (Abdul-Manan et al., 1999). WASp-WA also binds to WASp GBD, and GTP-Cdc42 competes for this binding site (Miki et al., 1998; Kim et al., 2000). Finally, Cdc42 enhances the ability of full-length recombinant N-WASP to activate Arp2/3 complex in vitro, an effect which is enhanced by PIP_2 (Rohatgi et al., 1999).

However, results obtained using recombinant full-length WASp or N-WASP to activate Arp2/3 complex in vitro are inconsistent. First, in all published experiments, WASp or N-WASP displayed considerable Arp2/3 complex activation ability in the absence of Cdc42, ranging from full constitutive activity of WASp (Yarar et al., 1999) to partial activity of N-WASP (Egile et al., 1999; Rohatgi et al., 1999). Second, Rohatgi et al. (1999) found that both GTP- and GDP-Cdc42 activated N-WASP, whereas Egile et al. (1999) showed that only GTP-Cdc42 was activated. Finally, lipid modification of Cdc42 varied in these studies as Rohatgi et al. (1999) used insect cell–expressed, prenylated Cdc42, whereas Egile et al. (1999) used *Escherichia coli*–expressed, unprenylated Cdc42. Both forms stimulated N-WASP. Attention to prenylation is significant since studies with cell extracts suggest that prenylated Cdc42 is required to activate actin polymerization (Zigmond et al., 1997; Ma et al., 1998a).

These inconsistencies leave open many questions regarding the mechanism of WASp or N-WASP activation by Cdc42. In principle, autoinhibition should be very tight to prevent activation of Arp2/3 complex in the absence of GTP-Cdc42, as observed in cell extracts. Also, the requirement for GTP-bound Cdc42 should be absolute since experiments in both whole cells and cell extracts suggest that GDP-Cdc42 is inactive (Nobes and Hall, 1995; Zigmond et al., 1997). For these reasons, we purified native WASp for the first time and studied its ability to activate Arp2/3 complex in the presence and absence of Cdc42 and PIP_2. We find that the regulation of WASp by PIP_2 and GTP-Cdc42 is robust, with WASp being inactive in their absence. PIP_2 alone stimulates WASp, whereas GTP-Cdc42 alone does not. However, GTP-Cdc42 does augment PIP_2 stimulation. This augmentation requires that Cdc42 be both GTP-bound and prenylated. The synergy between PIP_2 and GTP-Cdc42 causes WASp-mediated actin nucleation on lipid surfaces.

Materials and Methods

Protein Preparation

We purified Arp2/3 complex from bovine thymus following the method described in Higgs et al. (1999). Rabbit skeletal muscle actin was purified from acetone powder (Spudich and Watt, 1971), gel filtered (MacLean-Fletcher and Pollard, 1980), and labeled with pyrenyliodoacetamide (Pollard and Cooper, 1984).

GST WASp-WA and WASp-WA were prepared as previously described (Higgs et al., 1999). WASp152-309 was produced by expression in PET15b (Novagen), purification by nickel-NTA affinity chromatography (QIAGEN), and cleavage of the 6xHis tag with thrombin. Human Cdc42 was expressed in SF9 cells as a glutathione-S-transferase (GST) fusion protein in pAcGHLT (PharMingen) using the baculovirus expression system, and was purified from the membrane fraction by glutathione-Sepharose affinity chromatography with subsequent cleavage of the GST moiety (Heyworth et al., 1993). Human Cdc42 was expressed in *E. coli* as a GST fusion protein in pGEX-2T, and purified from the nonmembrane fraction by glutathione-Sepharose affinity chromatography and cleavage of GST (Heyworth et al., 1993). Cdc42 was charged with GTPγS or GDPβS by incubating 50 μM Cdc42 with 2.7 mM nucleotide in 10 mM Tris-HCl, pH 7.5, 1 mM DTT, 3 mM diethylenetrinitrilo-pentaaacetic acid, 0.5 mM $MgCl_2$ for 10 min at 30°C. $MgCl_2$ was added to 4 mM, the mixture was kept on ice and used within 2 h. This nucleotide exchange procedure was used because the high concentration of EDTA used in other procedures (Heyworth et al., 1993) accelerated actin polymerization from monomers in the pyrene-actin assay.

Antibody Production

The WASp 209-226 peptide was synthesized with an added cysteine residue at its NH_2 terminus on an Applied Biosystems 432A peptide synthesizer and coupled to keyhole limpet hemocyanin following instructions from the Pierce Chemical Co. This material was used to raise polyclonal antiserum in New Zealand white rabbits. AB1 was affinity-purified from serum using 209–226 peptide immobilized on Sulfolink gel (Pierce Chemical Co.).

WASp Concentration in Human Polymorphonuclear Leukocytes (PMN)

Human PMN were isolated from freshly drawn blood from healthy donors (The General Clinical Research Center, Scripps Research Institute) in ACD (Higgs et al., 1999). The cell number was determined using a hemacytometer. Cells (final concentration, 2.3×10^4 cells/μl) were added to boiling SDS-PAGE sample buffer and were boiled for 5 min. Protein concentration was 1 mg/ml by Bradford assay on a parallel sample diluted into 0.1% Thesit (Roche Biochemicals). The sample in SDS-PAGE buffer was diluted to various concentrations in the absence or presence of various concentrations of WASp152-309 in SDS-PAGE buffer. Samples were separated by SDS-PAGE and analyzed by Western blotting against AB1 with chemiluminescence detection. The integrated densities of the WASp and WASp152-309 bands were determined using NIH Image 1.60/ppc. Signals were linear for WASp between 1 and 10 μg PMN homogenate, and for WASp152-309 between 2.5 and 20 ng in a background of 5 μg PMN homogenate (44 pg protein/PMN determined by Bradford assay). WASp was determined to be 10.2 ng in 5 μg PMN homogenate from the WASp152-309 standard curve. WASp in 2.5 and 7.5 μg PMN homogenate was 4.8 and 16.2 ng, respectively. WASp concentration in PMN cytoplasm was determined using 1.8×10^{-13} liters/cell, in which the nuclear and granule volumes have been subtracted from the total cell volume (Ting-Beall et al., 1993).

WASp Purification

All steps were carried out at 4°C or on ice. All chromatographic supplies were purchased from Amersham Pharmacia Biotech. Six frozen bovine calf thymi (PelFreeze) were broken into small bits with a hammer, and homogenized in a blender followed by a Polytron (Bransonic) in 1 ml/g of EB (40 mM Tris-HCl, pH 8.0, 5 mM EGTA, 1 mM $MgCl_2$, 1 mM DTT, 1 mM PMSF, 20 μg/ml leupeptin, 6 μg/ml pepstatin A). The homogenate was centrifuged at 11,000 *g* for 15 min, and the resulting supernatant was centrifuged at 100,000 *g* for 1 h to obtain a high speed supernatant (HSS). The conductivity of the HSS was adjusted to the equivalent of QA (20 mM Tris-HCl, pH 8.0, 100 mM NaCl, 1 mM EGTA, 1 mM $MgCl_2$, 1 mM DTT, 2 μg/ml leupeptin, 2 μg/ml pepstatin A) with solid NaCl. The HSS was loaded onto 300 ml of Q Sepharose Fast Flow, and WASp was eluted with 3,000 ml of linear gradient to QB (QA + 200 mM NaCl). Fractions containing full-length WASp (by Western blot) were pooled and solid ammonium sulfate (GIBCO BRL) was added to 40% saturation (243 g/liter)

with vigorous mixing. After 15 min, the sample was centrifuged at 10,000 rpm for 15 min, and the pellet was redissolved in PB (20 mM Tris-HCl, pH 8.0, 1 mM EGTA, 1 mM $MgCl_2$, 1 mM DTT). The conductivity was adjusted to the equivalent of PA (PB + 1,000 mM NaCl), and the sample was loaded onto 50 ml of phenyl-Sepharose high performance equilibrated with PA. WASp was eluted with a linear gradient to PB. WASp-containing fractions were pooled, dialyzed against SA (10 mM Pipes, pH 6.8, 50 mM NaCl, 1 mM EGTA, 1 mM $MgCl_2$, 1 mM DTT), and loaded onto a MonoS 10/10 column equilibrated in SA. WASp was eluted with a linear gradient from SA to SB (SA + 500 mM NaCl). WASp-containing fractions were pooled and loaded onto a 1.6 × 60-cm Superdex200 column equilibrated in QA. WASp-containing fractions were pooled and concentrated by loading onto a MonoQ5/5 column equilibrated in QA and eluting with a linear gradient to QB. Sedimentation equilibrium ultracentrifugation of 40 nM bovine WASp in 10 mM imidazole, pH 7.0, 50 mM KCl, 1 mM $MgCl_2$, 1 mM EGTA, and 1 mM DTT at 23°C was carried out in a Beckman Optima XL-I. WASp sedimentation was monitored at 225 nm. Distributions of WASp at equilibrium were fitted using the nonlinear least squares method of Winnonln (Johnson et al., 1981).

Actin Polymerization by Fluorescence Spectroscopy

A detailed procedure is described in Higgs et al. (1999). Reactions contained 4 μM Mg-ATP actin (5% pyrene-labeled), 10 mM imidazole, pH 7.0, 50 mM KCl, 1 mM EGTA, and 1 mM $MgCl_2$ in G buffer-Mg (2 mM Tris-HCl, pH 8.0, 0.5 mM DTT, 0.2 mM ATP, 0.1 mM $MgCl_2$, 0.02% wt/vol NaN_3). When used, PIP_2 was added from a 2-mM stock in water. Pyrene fluorescence data (excitation at 365 nm and emission at 407 nm) were collected on a PTI AlphaScan spectrofluorometer (Photon Technology International) at a rate of 1 point/s. The concentration of filament ends (Ends) was determined at the point on the polymerization curve at which 80% of the actin had polymerized because few filaments form after this point (Higgs et al., 1999).

Phospholipid Vesicles

All phospholipids were suspended in chloroform and purchased from Avanti Polar Lipids including the following: egg phosphatidylcholine (PC); egg phosphatidylethanolamine (PE); brain phosphatidylserine (PS); brain phosphatidylinositol (PI); egg phosphatidic acid (PA); brain PIP_2; carboxyfluorescein-labeled PE (CF-PE); and cholesterol. For microscopy, lipids were mixed in the appropriate quantities, and the chloroform was removed under vacuum. The lipid film was resuspended in 10 mM imidazole, pH 7.0, 50 mM KCl, 1 mM EGTA, 1 mM $MgCl_2$ by vortexing, and subjected to five freeze/thaw cycles in dry ice/ethanol and a 37°C water bath. For vesicle pelleting assays, the same procedure was followed except: 0.05% di-bodipy-PC (Molecular Probes) was added to the lipids; 170 mM sucrose was added to the resuspension buffer; and the vesicles were extruded 10 times through 0.1-μm pore size polycarbonate filters (Lipex). Pelleting assays were conducted by mixing 2 μM WASp152-309 with unilamellar vesicles (500 μl total lipid) for 5 min at 23°C, and then centrifuging in a TLA-100 rotor (Beckman Coulter) for 15 min at 90,000 rpm. For all lipid mixtures, >99% of the lipid was in the pellet as judged by the depletion of di-bodipy-PC fluorescence from the supernatant. Pellets and supernatants were analyzed by SDS-PAGE and Coomassie staining.

Fluorescence Microscopy

Nucleation reactions were initiated as described above with 4 μM rhodamine-labeled phalloidin (Sigma Chemical Co.). After incubation at 23°C for 20 min, reactions were diluted either 625-fold (micelle experiments) or 25-fold (vesicle experiments) into microscopy buffer (50 mM KCl, 1 mM $MgCl_2$, 100 mM DTT, 20 μg/ml catalase, 100 μg/ml glucose oxidase, 3 mg/ml glucose, 0.5% methylcellulose, 10 mM imidazole, pH 7.0). Diluted sample (2 μl) was applied to coverslips coated with 0.1% nitrocellulose, and fluorescence was viewed with an Olympus X-70 microscope (Blanchoin et al., 2000).

Fluorescence Anisotropy

Experiments were conducted as previously described (Blanchoin and Pollard, 1998; Vinson et al., 1998). In brief, 0.1 μM of rhodamine-labeled WASp WA and varying concentrations of binding partners were incubated in 10 mM imidazole, pH 7.0, 50 mM KCl, 1 mM $MgCl_2$, 1 mM EGTA, and 0.025% Thesit (Roche Biochemicals) for 10 min at 23°C. Fluorescence anisotropy was measured in an AlphaScan spectrofluorometer (Photon Technologies International) at 552 nm excitation and 574 nm emission.

Results

Characterization of Antibodies Against WASp

Antibodies against a peptide consisting of residues 209–226 of human WASp, a region with no significant homology to N-WASP or Scar proteins, recognized a 65-kD band in lysates of human neutrophils and bovine thymus (Fig. 1 B). Although the calculated molecular mass of WASp is

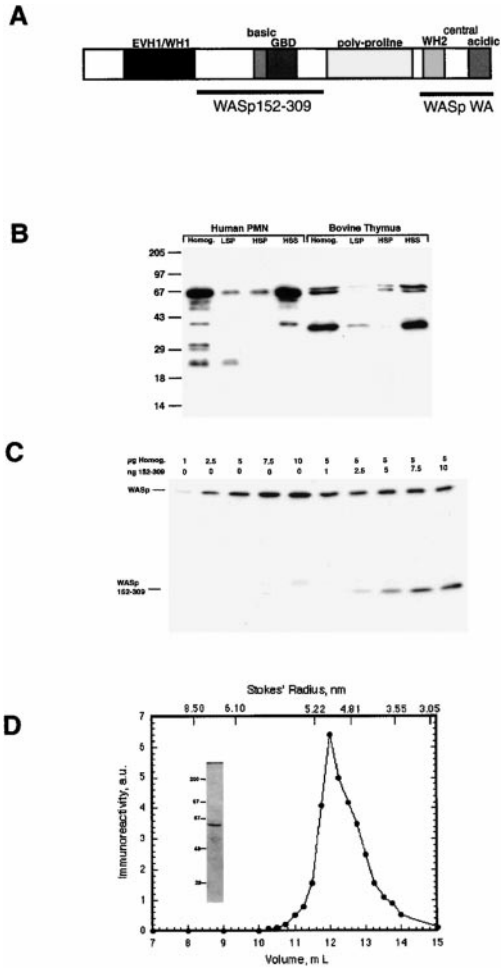

Figure 1. Extraction and purification of WASp from leukocytes. (A) Schematic diagram of WASp with the domains and constructs used in this study. (B) Extraction of WASp. Homogenates (Homog.) from human peripheral neutrophils and bovine thymus were fractionated into a 4,000-*g* pellet (LSP), 100,000-*g* pellet (HSP), and 100,000-*g* supernatant (HSS). 10 μg of the total homogenate and equal volumes of the centrifuged fractions were Western blotted with AB1. (C) Determination of WASp concentration in human neutrophils. SDS-PAGE of homogenates at various dilutions in the absence or presence of varying concentrations of WASp152-309. Western blots against AB1 were analyzed by densitometry. (D) Gel filtration of purified WASp on Superdex200 in 10 mM imidazole, pH 7.0, 50 mM KCl, 1 mM $MgCl_2$, 1 mM EGTA, and 1 mM DTT. The concentrations of WASp in the eluted fractions were measured by quantitative Western blotting. (inset) Coomassie blue–stained SDS-PAGE of 0.2 μg purified WASp before gel filtration.

53,041 D, migration of the band at 65 kD agrees with previous studies (Zhu et al., 1996). WASp from thymus migrated as a doublet, which might be due to limited proteolysis or to posttranslational modification. AB1 also reacted with several lower molecular mass bands, the most prominent in thymus at 40 kD, which varied in intensity between preparations. Several of these bands may be proteolytic fragments of full-length WASp since they were reduced by stringent regimes of protease inhibitors and they increased in lysates over time as the full-length WASp band decreased.

Most of the full-length WASp in these lysates partitioned into the 100,000-*g* supernatant, with minor amounts in the 4,000-*g* pellet and 100,000-*g* pellet (Fig. 1 B). The concentration of WASp in PMN cytoplasm was determined to be 9 ± 2 μM (Fig. 1 C), a value similar to the concentration of Arp2/3 complex in PMN (Higgs et al., 1999).

Purification and Physical Properties of WASp

We purified WASp from the 100,000-*g* supernatant of bovine calf thymus by anion exchange chromatography, ammonium sulfate precipitation, phenyl-Sepharose chromatography, and cation exchange chromatography, assessing purification steps by Western blotting. Although the yield of WASp was consistent among three preparations (8, 10, and 14 μg), the purity varied. After SDS-PAGE, one preparation yielded only one visible band by Coomassie staining (Fig. 1 D, inset). The other two preparations contained minor contaminating bands, none of which reacted with AB1. Purified WASp from all preparations had a Stokes' radius of 5.0 nm on Superdex 200 gel filtration chromatography (Fig. 1 D), which is considerably larger than that expected for a globular protein of 55 kD. By sedimentation equilibrium analytical ultracentrifugation, 40 nM native WASp had a molecular mass of 122 kD (not shown). The data were noisy owing to the low concentration of WASp, but rule out a monomer. Larger quantities will be required to determine if WASp is a dimer or a trimer.

We also attempted to purify the WASp expressed in insect cells using the baculovirus infection system. Despite good expression, we were unable to recover purified WASp using the native WASp purification procedure. A majority of recombinant WASp pelleted at low speed in the extract, and remained insoluble upon detergent and salt treatment. Furthermore, the WASp expressed in insect cells eluted heterogeneously from all columns, in contrast to the native WASp, which eluted as a single peak from each column. One possibility is that the WASp expressed in insect cells was in heterogeneous aggregates that caused it to fractionate poorly.

Effect of WASp, Cdc42, and PIP_2 on Actin Nucleation through Arp2/3 Complex

We tested the ability of full-length WASp to activate actin nucleation through Arp2/3 complex using fluorescence of pyrene-actin to follow the polymerization time course. WASp alone (4 nM) or with 10 nM Arp2/3 complex had no effect on the time course of actin polymerization (Fig. 2 A). The addition of 500 nM GTPγS-Cdc42 to WASp and Arp2/3 complex did not alter the polymerization time

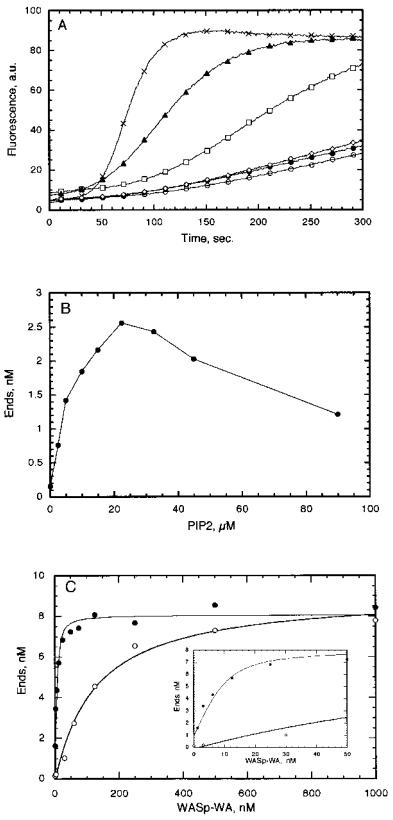

Figure 2. Activation of Arp2/3 complex by native WASp and WASp-WA. (A) Effect of Cdc42 and PIP_2 on WASp activation of Arp2/3 complex. Monomeric MgATP actin (4 μM, 5% pyrene-labeled) was polymerized in the presence of 10 nM of Arp2/3 complex and no addition (open circles), 4 nM WASp (filled circles), 4 nM WASp, and 500 nM prenylated GTPγS-Cdc42 (open diamonds), 4 nM WASp, and 20 μM PIP_2 micelles (open squares), 4 nM WASp, 20 μM PIP_2 micelles and 500 nM prenylated GTPγS-Cdc42 (filled triangles), and 500 nM WASp WA (crosses). (B) Dependence of nucleation by Arp2/3 complex and native WASp on PIP_2 concentration. Conditions were as described in A, with 4 nM WASp and a varying concentration of PIP_2 in the absence of Cdc42. The concentration of filament ends was calculated from the slopes of polymerization curves at 80% polymerization. (C) Dependence of nucleation by Arp2/3 complex on the concentrations of dimeric GST-WA (closed circles) or monomeric WASp-WA (open circles). Conditions are as in A, except no PIP_2 or Cdc42 was added.

course. However, addition of PIP_2 micelles to WASp and Arp2/3 complex accelerated polymerization and produced 12-fold more filaments (Fig. 2, A and B, and Table I). The addition of GTPγS-Cdc42 doubled the effect of PIP_2 alone. This synergy between PIP_2 and Cdc42 required GTPγS and recombinant Cdc42 from insect cells, which contained the prenyl modification (prenylated Cdc42). The Cdc42 expressed in *Escherichia coli* (unprenylated Cdc42) was inactive, as was prenylated GDPβS-Cdc42 (Table I). The effects of PIP_2 and prenylated GTPγS-Cdc42 required Arp2/3 complex and WASp. Neither PIP_2 nor prenylated GTPγS-Cdc42 changed the ability of WASp WA, the constitutively active COOH-terminal 70 residues of WASp, to activate Arp2/3 complex (not shown).

The degree to which WASp activated Arp2/3 complex

Table I. Effect of WASp Activators on Actin Nucleation by WASp and Arp2/3 Complex

Conditions	Concentration ends	Relative concentration ends
	nM	
Actin	0.13	1
Actin, Arp2/3 complex	0.13	1
Actin, Arp2/3 complex, WASp	0.15	1.2
Actin, Arp2/3 complex, WASp, PIP_2	1.57	12.1
Actin, Arp2/3 complex, WASp, prenylated GTPγS-Cdc42	0.15	1.2
Actin, Arp2/3 complex, WASp, PIP_2, prenylated GTPγS-Cdc42	2.99	23.0
Actin, Arp2/3 complex, WASp, PIP_2, unprenylated GDPβS-Cdc42	1.55	12.1
Actin, Arp2/3 complex, WASp, PIP_2, unprenylated GTPγS-Cdc42	1.08	8.3
Actin, Arp2/3 complex, WASp-WA	7.50	57.7

Reagent concentrations: 4 μM actin, 10 nM Arp2/3 complex, 4 nM WASp, 20 μM PIP_2, 0.5 μM Cdc42, and 1 μM WASp-WA. Concentration ends were determined at 80% polymerization (Higgs et al., 1999).

in the absence of prenylated GTPγS-Cdc42 and PIP_2 varied slightly among the three WASp preparations. Two of the preparations displayed no activation ability, whereas the third stimulated a twofold increase in filaments nucleated in the absence of activators. However, all three preparations responded in near identical fashion to activation by PIP_2 and prenylated GTPγS-Cdc42.

Native WASp was remarkably active in the presence of PIP_2 and prenylated GTPγS-Cdc42. At 4 nM, WASp generated 3-nM filaments (Table I). At the same concentration, WASp-WA had no detectable effect on polymerization (Fig. 2 C). To investigate whether the multimeric state of full-length WASp contributes to this high activity, we tested dimeric GST WASp-WA. Dimeric GST-WA was almost 100-fold more efficient at activating Arp2/3 complex than monomeric WA, resulting in activation similar to activated native WASp (Fig. 2 C).

Actin Networks Generated by WASp and Arp2/3 Complex

We next examined the effect of WASp on Arp2/3 complex–mediated actin networks by fluorescence microscopy (Blanchoin et al., 2000). In the presence of Arp2/3 complex, WASp alone (from the partially active preparation) induced a greater number of shorter filaments than Arp2/3 complex alone (Fig. 3 C and Table II), but created few branches. The addition of prenylated GTPγS-Cdc42 did not change filament length or the degree of branching (Fig. 3 E and Table II). The addition of PIP_2 to WASp and Arp2/3 complex dramatically increased the number of branches and reduced the mean filament length (Fig. 3 D and Table II) because of the more complete activation of Arp2/3 complex by the limiting quantity of WASp (Higgs et al., 1999; Blanchoin et al., 2000). PIP_2 and prenylated GTPγS-Cdc42 with WASp and Arp2/3 complex produced highly fluorescent halos of actin filaments (Fig. 3 F). These halos, which were much larger (diameter of 7.2 ± 3.1 μm, $n = 25$) than the 10-nm diam PIP_2 micelles, did not represent the majority of the polymerized actin, but were clearly sites of intense nucleation. Unprenylated GTPγS-Cdc42 did not generate actin filament halos with PIP_2, WASp, and Arp2/3 complex (not shown). Because of the intense fluorescence of the halos, individual filaments were hard to resolve. Those that could be resolved were not heavily branched, and the branches were oriented randomly with respect to the halo (out of six discernible branches, three branched toward the halo and three away from it). The halos were unstable and rapidly shed filaments upon prolonged exposure to the halogen lamp, sometimes resulting in exploding halos. The shed filaments were short (<2 μm) and highly branched. Filaments distant from the halos appeared to exist in two populations: long unbranched filaments and short branched filaments (Table II). These results suggest that aggregates consisting of PIP_2 micelles and prenylated GTPγS-Cdc42 serve as activation centers for WASp. These effects depended on both GTPγS and prenylation of Cdc42.

Multilamellar vesicles containing 10% PIP_2 also stimulated the formation of filament-rich halos, providing prenylated GTPγS-Cdc42 was also present (Fig. 3 H). These halos of actin filaments, similar in size (8.1 ± 3.8–μm diam, $n = 52$) to those forming around micelles, had a vesicle at their core, revealed using vesicles containing 5% fluorescein-PE (Fig. 3 H, inset). Only ~10% of the fluorescent vesicles were surrounded by actin, possibly because of nonuniform distribution of prenylated GTPγS-Cdc42 on the vesicles. In contrast to the micelle experiments, most of the fluorescent actin filaments were associated with vesicles. Few filaments were >20 μm from the filament-encircled vesicles. Filaments dissociated from the halos over time (not shown), suggesting that filaments not associated with vesicles were probably nucleated from the vesicle and then dissociated. Actin filaments also polymerized around PS-containing vesicles in the presence of GTPγS-Cdc42-BV, WASp, and Arp2/3 complex (Fig. 3 G). Although the mean sizes of these actin-containing structures were comparable (7.4 ± 3.7 μm, $n = 11$), they were 40-fold less abundant than the actin-surrounded PIP_2 vesicles and did not represent the majority of polymerized actin. PIP_2-containing vesicles with WASp and Arp2/3 complex without Cdc42 produced many short, highly branched filaments (not shown), indicating increased actin nucleation. However, these actin filaments did not cluster around vesicles. In summary, both prenylated GTPγS-Cdc42 and PIP_2 were required to produce actin filament–rich foci around micelles and vesicles.

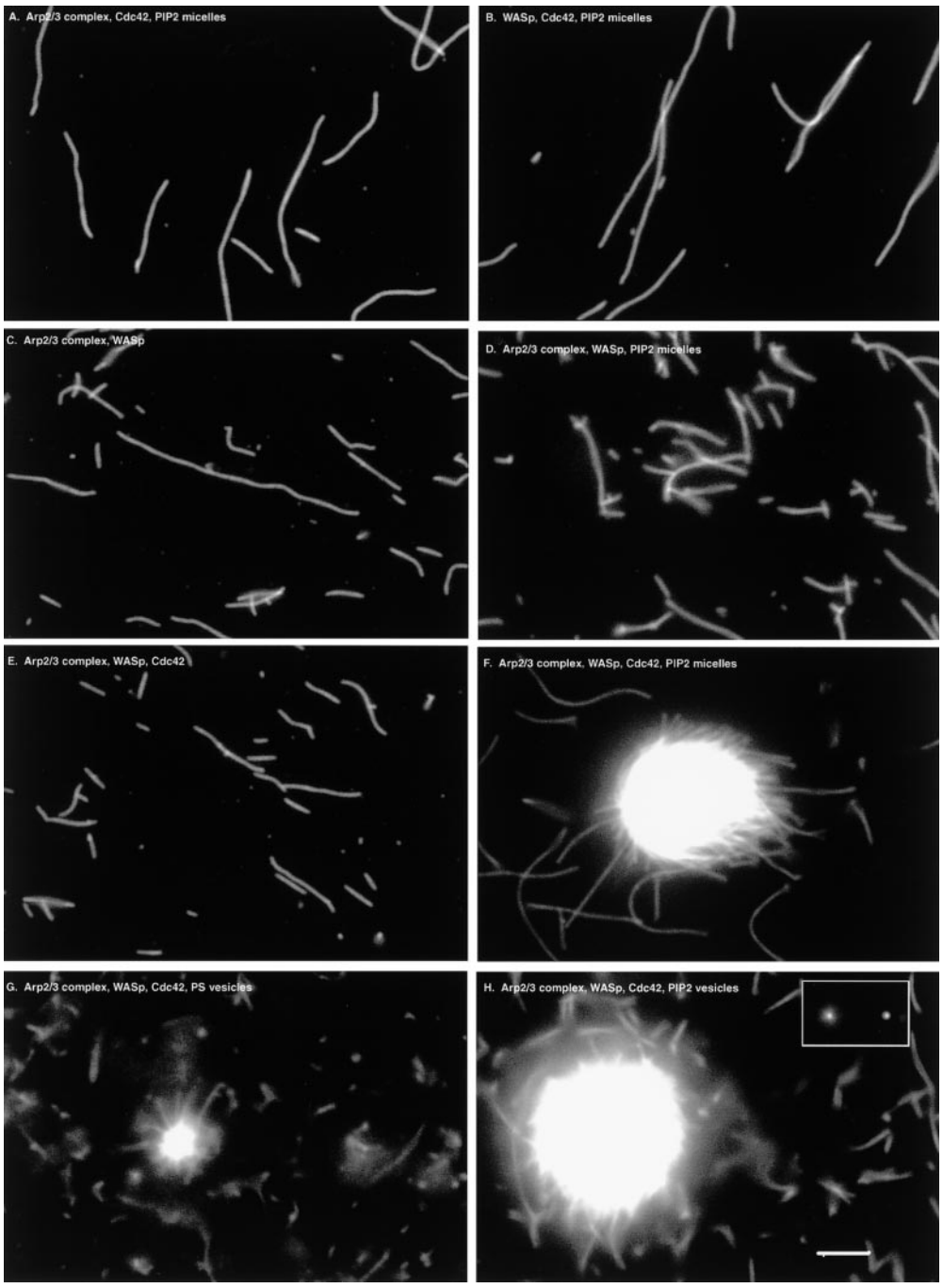

Figure 3. Fluorescence micrographs of the products of actin polymerization reactions. Polymerization reactions contained 4 μM monomeric MgATP actin, with or without 100 nM of Arp2/3 complex, 4 nM WASp, 0.5 μM prenylated GTPγS-Cdc42, 22 μM PIP_2 micelles, or 100 μM of phospholipid vesicles. After polymerization for 20 min at 23°C in KMEI containing 4 μM rhodamine-phalloidin, samples were diluted 625-fold (A–F) or 25-fold (G and H) into motility buffer, mounted on nitrocellulose-coated coverslips, and viewed with filters for rhodamine. (A) Arp2/3 complex, prenylated GTPγS-Cdc42, PIP_2 micelles, (B) WASp, prenylated GTPγS-Cdc42, PIP_2 micelles, (C) Arp2/3 complex, WASp, (D) Arp2/3 complex, WASp, PIP_2 micelles, (E) Arp2/3 complex, WASp, prenylated GTPγS-Cdc42, (F) Arp2/3 complex, WASp, prenylated GTPγS-Cdc42, PIP_2 micelles, (G) Arp2/3 complex, WASp, prenylated GTPγS-Cdc42, multilamellar vesicles containing 50% cholesterol/14.5% PC/14.5% PE/20% PS/1% CF-PE, or (H) Arp2/3 complex, WASp, prenylated GTPγS-Cdc42, multilamellar vesicles containing 50% cholesterol/19.5% PC/19.5% PE/10% PIP_2/1% CF-PE. Inset in G shows corresponding fluorescein image of G, showing the vesicle at the interior of the actin halo (left) and a vesicle not surrounded by actin.

Table II. Quantitative Analysis of Polymerization Products

Conditions	Filament length		No filaments (unbranched/branched)	Percent branched
	unbranched	branched		
	μm ± SD			
Arp2/3 complex, prenylated GTPγS-Cdc42, PIP_2	7.0 ± 6.5		105/1	1
WASp, prenylated GTPγS-Cdc42, PIP_2	6.6 ± 6.2		140/1	1
Arp2/3 complex, WASp	2.6 ± 1.9		125/2	2
Arp2/3 complex, PIP_2	3.2 ± 2.6	1.5 ± 1.3	101/37	27
Arp2/3 complex, WASp, prenylated GTPγS-Cdc42	2.7 ± 1.8		87/1	1
Arp2/3 complex, WASp, prenylated GTPγS-Cdc42, PIP_2	7.2 ± 4.1	1.5 ± 1.4	127/92	42

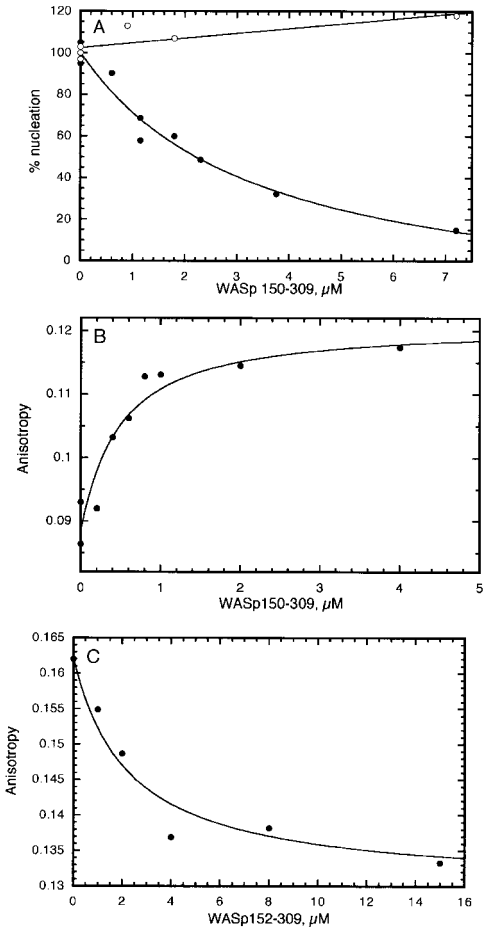

Figure 4. Regulation of WASp-WA by a fragment of WASp including the GBD. (A) WASp 152-309 inhibits Arp2/3 complex activation by WASp WA. Nucleation reactions included 4 μM of monomeric MgATP actin (5% pyrene-labeled), 10 nM of Arp2/3 complex, 250 nM WASp WA or Scar1 WA, and varying concentrations of WASp 152-309. The concentration of filament ends created by Arp2/3 complex was calculated from the slope of the polymerization curve at 80% polymerization. Percent nucleation is the concentration of ends created relative to that created by Arp2/3 complex and WASp WA or Scar1 WA in the absence of WASp 152-309, after subtraction of the concentration of filaments created in the absence of WA. (B) Binding of WASp 152-309 to WASp WA was measured by fluorescence anisotropy of rhodamine-labeled WASp WA (0.1 μM). The calculated dissociation equilibrium constant is 0.42 μM. (C) Fluorescence anisotropy assay for competition between Arp2/3 complex and WASp152-309 for binding WASp WA. Rhodamine-labeled WASp WA (0.1 μM) has an anisotropy of 0.162 when bound to 1 μM of Arp2/3 complex. The smaller WASp152-309 competes off Arp2/3 complex, giving an anisotropy of 0.132.

Effect of WASp GBD on WASp WA Activity

Our finding that native WASp does not activate Arp2/3 complex unless stimulated by PIP_2 and prenylated GTPγS-Cdc42 supports an autoinhibition mechanism for WASp (Miki et al., 1998; Kim et al., 2000). We tested the possibility that NH_2-terminal WASp motifs bind the WA region and prevent it from activating Arp2/3 complex using a construct of WASp (termed WAS p152-309) expressed in *E. coli*. This construct begins immediately after the predicted EVH1 domain and ends just before the polyproline region (Fig. 1 A). Thus, WASp152-309 contains the entire WASp GBD as well as residues essential for binding WASp-WA (Kim et al., 2000).

The addition of WASp152-309 to nucleation reactions containing 0.25 μM WASp-WA and 10 nM Arp2/3 complex inhibited filament production, with half-maximal inhibition at 3 μM (Fig. 4 A). Importantly, WASp152-309 did not inhibit nucleation by Scar1-WA and Arp2/3 complex, as predicted, because residues of WASp-WA that bind WASp GBD (Kim et al., 2000) are completely different from the corresponding part of Scar1 WA. In a fluorescence anisotropy assay, WASp152-309 bound WASp-WA with a dissociation equilibrium constant of 0.42 μM (Fig. 4 B). WAS p152-309 also inhibited binding of Arp2/3 complex to rhodamine WASp-WA (Fig. 4 C), suggesting that WAS p152-309 inhibits nucleation by interfering with WASp-WA binding to Arp2/3 complex.

Both prenylated GTPγS-Cdc42 (Fig. 5 A) and unprenylated GTPγS-Cdc42 (not shown) overcame the inhibition

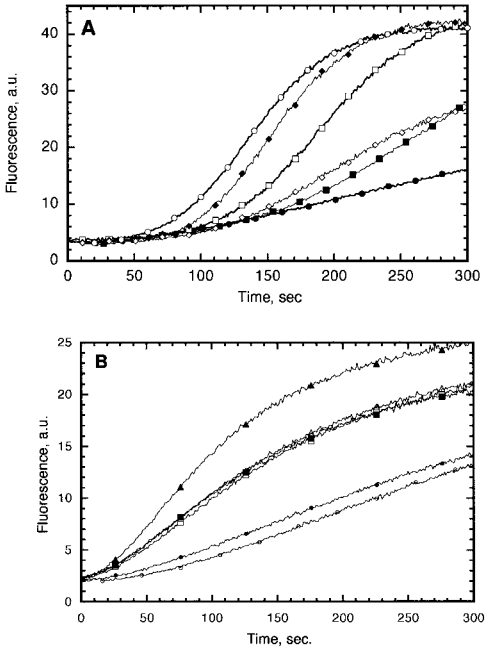

Figure 5. WASp152-309 interacts with GTPγS-Cdc42 but not with PIP_2. (A) Effect of GTPγS-Cdc42 and PIP_2 on nucleation inhibition by WASp152-309. Nucleation assays were performed as described in Fig. 2 A with 10 nM of Arp2/3 complex alone (filled circles); Arp2/3 complex, 250 nM WASp WA (open circles); Arp2/3 complex, WASp WA, 3 μM WASp152-309 (filled squares); Arp2/3 complex, WASp WA, WASp152-309, 1.6 μM prenylated GTPγS-Cdc42 (open squares); Arp2/3 complex, WASp WA, WASp152-309, 3.2 μM prenylated GTPγS-Cdc42 (filled diamonds); and Arp2/3 complex, WASp WA, WASp152-309, 30 μM PIP_2 (open diamonds). (B) Effect of WASp152-309 on full-length native WASp activation by PIP_2 and GTPγS-Cdc42. Nucleation assays were performed as described in Fig. 2 A with 10 nM of Arp2/3 complex alone (open circles); Arp2/3 complex, 2 nM WASp (filled circles); Arp2/3 complex, WASp, 20 μM PIP_2 (open squares); Arp2/3 complex, WASp, PIP_2, 25 μM WASp152-309 (filled squares); Arp2/3 complex, WASp + PIP_2, 0.5 μM prenylated GTPγS-Cdc42 (filled triangles); and Arp2/3 complex, WASp, PIP_2, prenylated GTPγS-Cdc42, 25 μM WASp152-309 (open triangles).

of WASp-WA by WASp152-309 in the pyrene-actin nucleation assay, whereas PIP_2 did not reverse this inhibition. We also tested the effect of WASp152-309 on Arp2/3 complex activation by full-length WASp. WASp152-309 did not block the effect of PIP_2 on WASp, but did block the effect of prenylated GTPγS-Cdc42 (Fig. 5 B). These results suggest that WASp152-309 might not contain the region responsive to PIP_2. In support of this conclusion, WASp152-309 did not bind to vesicles containing PIP_2 or other anionic lipids (not shown).

Discussion

This is the first study to characterize native WASp from leukocytes in terms of its cellular fractionation, cellular concentrations, and ability to activate Arp2/3 complex. The concentration of WASp in human neutrophils is surprisingly high (9 μM), almost equal to that of Arp2/3 complex (Higgs et al., 1999). This high concentration of WASp suggests that its ability to activate Arp2/3 complex must be tightly regulated since, at this concentration, even a low constitutive activity would cause significant Arp2/3 complex activation.

Evidence from cell extract studies also suggests that Arp2/3 complex activation is tightly regulated, being strongly activated by GTP-Cdc42 and PIP_2 (Zigmond et al., 1997; Ma et al., 1998a; Mullins and Pollard, 1999). WASp and N-WASP are leading candidates for mediators of this activation. However, previous studies showed that low concentrations of WASp isolated from insect cells potently activated Arp2/3 complex in the absence of any activators (Yarar et al., 1999). Other studies using the N-WASP isolated from insect cells showed considerable constitutive Arp2/3 complex activation in the absence of activators (Egile et al., 1999; Rohatgi et al., 1999). In the latter two cases, the candidate WASp and N-WASP stimulator, Cdc42, did increase Arp2/3 complex activation, but surprisingly did so with both GDP- and GTP-bound in one study (Rohatgi et al., 1999). PIP_2 enhanced GTP-Cdc42 activation of N-WASP in one study (Rohatgi et al., 1999), but was not tested by Egile et al. The combination of these results suggests that the WASp and N-WASP expressed in insect cells is not as tightly regulated as expected for the activator of Arp2/3 complex.

Our results with native WASp activating Arp2/3 complex differ in two ways from previous work on WASp and N-WASP expressed in insect cells (Egile et al., 1999; Rohatgi et al., 1999; Yarar et al., 1999). First, the difference in Arp2/3 complex activation between nonactivated and fully activated WASp is much greater in our study. Second, PIP_2 micelles alone stimulate native WASp, whereas prenylated GTPγS-Cdc42 alone does not at 0.5 μM. However, we found that prenylated GTPγS-Cdc42 increased WASp stimulation by PIP_2 twofold. Cdc42 had to be GTPγS-bound and prenylated for this effect.

In our hands, the WASp expressed in insect cells behaves in a heterogeneous fashion, but the WASp from bovine thymus and human neutrophils behaves much more homogeneously. Over 90% of WASp from extracts of either leukocyte source partitions into the 100,000-*g* supernatant, indicating that the majority is not associated with either the actin cytoskeleton or membranes under these conditions. This also suggests that most WASp molecules are not bound to GTP-Cdc42 or to PIP_2 because both of these ligands are associated with the membranes (Regazzi et al., 1992; Nomanbhoy et al., 1999). Purified WASp has a Stokes' radius of 5.0 nm by gel filtration, and a mass of 122 kD by sedimentation equilibrium analytical ultracentrifugation. Because no other bands were visible in the cleanest WASp preparation, the size suggests that WASp is a multimer, either a dimer or a trimer. The WASp multimer appears to be very stable, since only 40 nM of WASp was used for these analytical techniques. Others have proposed N-WASP to be a multimer, with a sedimentation coefficient of 5.45 S at 1 μM, by sedimentation velocity analytical ultracentrifugation (Carlier et al., 2000). These authors also proposed that N-WASP is in equilibrium between monomer and multimer, and that the monomer is the active state. Our results at 40 nM WASp suggest that the equilibrium strongly favors the multimer. Further work is necessary to determine the stoichiometry of the multimer, the interfaces involved in multimerization, and the effects of WASp activators on the multimeric state.

When stimulated by both PIP_2 and prenylated GTPγS-Cdc42, native WASp activated Arp2/3 complex much more strongly than the constitutively active WA fragment. WASp at 4 nM activated Arp2/3 complex almost stoichiometrically, whereas 4 nM WA caused no detectable activation. Dimeric GST-WA had an activation efficiency similar to native WASp, and could fully activate Arp2/3 complex at a 50-fold lower concentration than WA. Dimeric GST-WA binds actin and Arp2/3 complex with an affinity similar to monomeric WA (Marchand, J.B., H.N. Higgs, and T.D. Pollard, unpublished data). The multimeric state of native WASp and GST-WA may contribute to a higher activation efficiency, but the mechanism is not yet clear.

Our observations suggest that the synergy between PIP_2 and Cdc42 is dependent on localization of both activators on a membrane surface. PIP_2 micelles or vesicles containing PIP_2 or PS were foci of intense actin filament nucleation in the presence of prenylated (but not unprenylated) GTPγS-Cdc42 and native WASp. When prenylated, Cdc42 stably associates with membranes (Nomanbhoy et al., 1999). This is similar to other particulate activators of Arp2/3 complex including bacteria (Welch et al., 1997b), viruses (Frischknecht et al., 1999), intracellular vesicles (Taunton et al., 2000), beads coated with bacterial or eukaryotic activators of Arp2/3 complex (Cameron et al., 1999; Yarar et al., 1999), or beads coated with Cdc42 (Ma et al., 1998b). Others have also observed Cdc42- and PIP_2-dependent vesicle movement in whole cell extracts (Ma et al., 1998a; Moreau and Way, 1998), although the minimum requirements for this effect could not be determined in these studies. Vesicles with PIP_2 were more effective in producing these actin halos than micelles of PIP_2 or vesicles containing PS. PIP_2-containing vesicles alone promote dendritic nucleation by native WASp and Arp2/3 complex, but the filaments do not concentrate around vesicles. We do not know at present whether actin filaments nucleated by WASp and Arp2/3 complex in the presence of prenylated GTPγS-Cdc42- and PIP_2-containing vesicles are associated noncovalently with the vesicle surface. If WASp binds actin filaments like N-WASP (Egile et al., 1999), some filaments may attach by this mechanism. However,

the actin filament halo is so thick around the vesicle that the majority of filaments are probably not bound to the membrane but held in place by the dendritic network formed during nucleation by Arp2/3 complex (Blanchoin et al., 2000).

Kim et al. (2000) proposed a mechanism for WASp regulation by GTP-Cdc42 based on earlier ideas on autoinhibition (Miki et al., 1998). A nuclear magnetic resonance structure and direct binding assays showed that WASp GBD binds to residues 461–492 of WASp-WA. This interaction was proposed to block binding of WASp-WA to Arp2/3 complex. Binding of GTP-Cdc42 to WASp GBD was proposed to release WASp-WA, allowing it to bind and activate Arp2/3 complex. Our experiments are consistent with the main features of this model. A construct (WASp152-309) containing the WASp GBD inhibited WASp WA activation of Arp2/3 complex by competing with Arp2/3 complex for WA binding. GTPγS-Cdc42 relieved inhibition by WASp152-309. Conversely, WASp152-309 blocked enhancement of native WASp stimulation by GTPγS-Cdc42. On the other hand, 0.5 μM prenylated GTPγS-Cdc42 alone does not overcome autoinhibition of native WASp since WA binds so tightly to WASp GBD that it reduces the affinity of the GBD for GTP-Cdc42 by 80–300-fold (Kim et al., 2000). To be an effective activator of WASp at a submicromolar concentration, prenylated GTPγS-Cdc42 requires a membrane containing an acidic lipid such as PIP_2. However, our results do not rule out other mechanisms acting in concert with or separately from the autoinhibition model as proposed.

The PIP_2 binding site on WASp is unknown. N-WASP and WASp were originally predicted to have an NH_2-terminal PH domain (Miki et al., 1996), but atomic structures revealed a polyproline binding EVH1 domain (Fedorov et al., 1999; Prehoda et al., 1999) that overlaps, but is offset from, the proposed PH domain. A polybasic region is present in WASp152-309 immediately NH_2-terminal to the WASp GBD. However, WASp152-309 did not block native WASp activation by PIP_2 nor did PIP_2 relieve WASp WA inhibition by WASp152-309. Additionally, WASp152-309 does not bind PIP_2-containing vesicles. These results suggest that WASp152-309 does not contain the complete PIP_2 binding site. Since WASp WA does not bind PIP_2 (not shown), PIP_2 binding may depend on the NH_2-terminal region or the region between GBD and WA. This site might not be specific for PIP_2 since PS-containing vesicles also cause actin halo formation.

The signaling pathway to WASp and Arp2/3 complex may operate through GTP activation of Cdc42 alone in the context of an anionic membrane surface, possibly containing PIP_2, as follows. Binding to anionic lipid on the membrane surface partially activates WASp, possibly by exposing the acidic COOH terminus of WASp that interacts with Arp2/3 complex. Interaction of WASp with anionic lipid may also allow GTP-Cdc42 to bind the WASp GBD, perhaps concentrating WASp together with prenylated Cdc42 on the membrane surface, reducing their interaction potential. Interaction with Cdc42 fully stimulates WASp to activate Arp2/3 complex by releasing WA. WASp binding to Cdc42 may also stabilize active WASp on the membrane, resulting in localized actin polymerization. Nonlipidated Cdc42 is ineffective since it does not bind vesicles.

Many aspects of this model remain to be tested including the following: the PIP_2 binding site on WASp; WASp affinity for PIP_2 and other lipids; the mechanism of partial WASp activation by PIP_2; and the equilibrium and rate constants for WASp association with membranes containing PIP_2 and/or Cdc42. Also, a full understanding of WASp activation will require accurate values for cellular concentrations of PIP_2 and GTP-Cdc42 upon cell stimulation in addition to the knowledge of distributions of these molecules in cells. The proposed synergism between GTP-Cdc42 and PIP_2, mediated by membrane binding, might provide a mechanism for the membrane-associated actin polymerization at the leading edge and on phagosomes/endosomes (Merrifield et al., 1999; Taunton et al., 2000). In addition, other WASp-binding proteins (Grb2, Nck, Src kinases, Btk) are membrane-associated upon cell stimulation, which might similarly affect WASp activation (Carlier et al., 2000; for review see Higgs and Pollard, 1999).

We thank Jean-Baptiste Marchand, Wei-Lih Lee, and Laurent Blanchoin for help and advice. We are grateful to Roberta Schulte and Bartholemew Sefton for help with the baculovirus expression system and for cloning and expressing WASp in this system. The DNA constructs for Cdc42, along with much helpful advice for their expression, as well as advice on handling neutrophils, were supplied by Gary Bokoch and colleagues at Scripps Research Institute. Jill Meisenhelder (Salk Institute Cancer Center) synthesized the WASp 209-226 peptide.

This work was supported by the National Institutes of Health (NIH) research grants GM-26338 (to T.D. Pollard) and CA-14195 (to Walter Eckhart), an NIH National Research Service Award Posdoctoral Fellowship to H.N. Higgs, NIH grant RR00833 to The General Clinical Research Center at Scripps Research Institute.

Submitted: 15 June 2000
Revised: 17 July 2000
Accepted: 18 July 2000

References

Abdul-Manan, N., B. Aghazadeh, G.A. Liu, A. Majumdar, O. Ouerfelli, K.A. Siminovitch, and M.K. Rosen. 1999. Structure of Cdc42 in complex with the GTPase-binding domain of the 'Wiskott-Aldrich Syndrome' protein. *Nature*. 399:379–383.

Bailly, M., F. Macaluso, M. Cammer, A. Chan, J.E. Segall, and J.S. Condeelis. 1999. Relationship between Arp2/3 complex and the barbed ends of actin filaments at the leading edge of carcinoma cells after epidermal growth factor stimulation. *J. Cell Biol.* 145:331–345.

Balasubramanian, M.K., A. Feoktistova, D. McCollum, and K.L. Gould. 1996. Fission yeast Sop2p: a novel and evolutionarily conserved protein that interacts with Arp3p and modulates profilin function. *EMBO (Eur. Mol. Biol. Organ.) J.* 15:6426–6437.

Blanchoin, L., and T.D. Pollard. 1998. Interaction of actin monomers with *Acanthamoeba* actophorin (ADF/cofilin) and profilin. *J. Biol. Chem.* 273: 25106–25111.

Blanchoin, L., K.J. Amann, H.N. Higgs, J.B. Marchand, D.A. Kaiser, and T.D. Pollard. 2000. Direct observation of dendritic actin filament networks nucleated by Arp2/3 complex and WASp/Scar proteins. *Nature*. 404:1007–1011.

Cameron, L.A., M.J. Footer, A. van Oudenaarden, and J.A. Theriot. 1999. Motility of ActA protein-coated microspheres driven by actin polymerization. *Proc. Natl. Acad. Sci. USA*. 96:4908–4913.

Carlier, M.F., P. Nioche, I. Broutin-L'Hermite, R. Boujemaa, C. Le Clainche, C. Egile, C. Garbay, A. Ducruix, P.J. Sansonetti, and D. Pantaloni. 2000. Grb2 links signalling to actin assembly by enhancing interaction of neural Wiskott-Aldrich Syndrome protein (N-WASP) with actin-related-protein (Arp2/3) complex. *J. Biol. Chem.* 275:21946–21952.

Egile, C., T.P. Loisel, V. Laurent, R. Li, D. Pantaloni, P.J. Sansonetti, and M.F. Carlier. 1999. Activation of the CDC42 effector N-WASP by the *Shigella flexneri* IcsA protein promotes actin nucleation by Arp2/3 complex and bacterial actin-based motility. *J. Cell Biol.* 146:1319–1332.

Fedorov, A.A., E. Fedorov, F. Gertler, and S.C. Almo. 1999. Structure of EVH1, a novel proline-rich ligand-binding module involved in cytoskeletal

dynamics and neural function. *Nat. Struct. Biol.* 6:661–665.
Frischknecht, F., V. Moreau, S. Rottger, S. Gonfloni, I. Reckmann, G. Superti-Furga, and M. Way. 1999. Actin-based motility of vaccinia virus mimics receptor tyrosine kinase signalling. *Nature*. 401:926–929.
Heyworth, P.G., U.G. Knaus, D.J. Xu, D.J. Uhlinger, L. Conroy, G.M. Bokoch, and J.T. Curnutte. 1993. Requirement for posttranslational processing of Rac GTP-binding proteins for activation of human neutrophil NADPH oxidase. *Mol. Biol. Cell*. 4:261–269.
Higgs, H.N., and T.D. Pollard. 1999. Regulation of actin polymerization by Arp2/3 complex and WASp/Scar proteins. *J. Biol. Chem.* 274:32531–32534.
Higgs, H.N., L. Blanchoin, and T.D. Pollard. 1999. Influence of the Wiskott-Aldrich syndrome protein (WASp) C terminus and Arp2/3 complex on actin polymerization. *Biochemistry*. 38:15212–15222.
Johnson, M.L., J.J. Correia, D.A. Yphantis, and H.R. Halvorson. 1981. Analysis of data from the analytical ultracentrifuge by nonlinear least-squares techniques. *Biophys. J.* 36:575–588.
Kim, A.S., L.T. Kakalis, N. Abdul-Manan, G.A. Liu, and M.K. Rosen. 2000. Autoinhibition and activation mechanisms of the Wiskott-Aldrich Syndrome protein. *Nature*. 404:151–158.
Ma, L., L.C. Cantley, P.A. Janmey, and M.W. Kirschner. 1998a. Corequirement of specific phosphoinositides and small GTP-binding protein Cdc42 in inducing actin assembly in *Xenopus* egg extracts. *J. Cell Biol.* 140:1125–1136.
Ma, L., R. Rohatgi, and M.W. Kirschner. 1998b. The Arp2/3 complex mediates actin polymerization induced by the small GTP-binding protein Cdc42. *Proc. Natl. Acad. Sci. USA*. 95:15362–15367.
Machesky, L.M., and R.H. Insall. 1998. Scar1 and the related Wiskott-Aldrich syndrome protein WASP regulate the actin cytoskeleton through the Arp2/3 complex. *Curr. Biol.* 8:1347–1356.
Machesky, L.M., S.J. Atkinson, C. Ampe, J. Vandekerckhove, and T.D. Pollard. 1994. Purification of a cortical complex containing two unconventional actins from *Acanthamoeba* by affinity chromatography on profilin agarose. *J. Cell Biol.* 127:107–115.
Machesky, L.M., E. Reeves, F. Wientjes, F.J. Mattheyse, A. Grogan, N.F. Totty, A.L. Burlingame, J.J. Hsuan, and A.W. Segal. 1997. Mammalian actin-related protein 2/3 complex localizes to regions of lamellipodial protrusion and is composed of evolutionarily conserved proteins. *Biochem J.* 328: 105–112.
Machesky, L.M., D.M. Mullins, H.N. Higgs, D.A. Kaiser, L. Blanchoin, R.C. May, M.E. Hall, and T.D. Pollard. 1999. Scar, a WASp-related protein, activates nucleation of actin filaments by the Arp2/3 complex. *Proc. Natl. Acad. Sci. USA*. 96:3739–3744.
MacLean-Fletcher, S., and T.D. Pollard. 1980. Identification of a factor in conventional muscle actin preparation which inhibits actin filament self-association. *Biochem. Biophys. Res. Commun.* 96:18–27.
Marchand, J.B., D.A. Kaiser, T.D. Pollard, and H.N. Higgs. 2000. Interaction of WASp/Scar proteins with actin and vertebrate Arp2/3 complex. *Nat. Cell Biol.* In press.
McCollum, D., A. Feoktistova, M. Morphew, M. Balasubramanian, and K.L. Gould. 1996. The *Schizosaccharomyces pombe* actin-related protein, Arp3, is a component of the cortical actin cytoskeleton and interacts with profilin. *EMBO (Eur. Mol. Biol. Organ.) J.* 15:6438–6446.
Merrifield, C.J., S.E. Moss, C. Ballestrem, B.A. Imhof, G. Giese, I. Wunderlich, and W. Almers. 1999. Endocytic vesicles move at the tips of actin tails in cultured mast cells. *Nat. Cell Biol.* 1:72–74.
Miki, H., K. Miura, and T. Takenawa. 1996. N-WASP, a novel actin-depolymerizing protein, regulates the cortical cytoskeletal rearrangement in a PIP_2-dependent manner downstream of tyrosine kinases. *EMBO (Eur. Mol. Biol. Organ.) J.* 15:5326–5335.
Miki, H., T. Sasaki, Y. Takai, and T. Takenawa. 1998. Induction of filopodium formation by a WASP-related actin-depolymerizing protein N-WASP. *Nature*. 391:93–96.
Moreau, V., and M. Way. 1998. Cdc42 is required for membrane dependent actin polymerization in vitro. *FEBS (Fed. Eur. Biochem. Soc.) Lett.* 427:353–356.
Morrell, J.L., M. Morphew, and K.L. Gould. 1999. A mutant of Arp2p causes partial disassembly of the Arp2/3 complex and loss of cortical actin function in fission yeast. *Mol. Biol. Cell*. 10:4201–4215.
Mullins, R.D., and T.D. Pollard. 1999. Rho-family GTPases require the Arp2/3 complex to stimulate actin polymerization in *Acanthamoeba* extracts. *Curr. Biol.* 9:405–415.
Mullins, R.D., J.A. Heuser, and T.D. Pollard. 1998. The interaction of Arp2/3 complex with actin: nucleation, high-affinity pointed end capping, and formation of branching networks of filaments. *Proc. Natl. Acad. Sci. USA*. 95: 6181–6186.
Nobes, C.D., and A. Hall. 1995. Rho, rac, and cdc42 GTPases regulate the assembly of multimolecular focal complexes associated with actin stress fibers, lamellipodia, and filopodia. *Cell*. 81:53–62.
Nomanbhoy, T.K., J.W. Erickson, and R.A. Cerione. 1999. Kinetics of Cdc42 membrane extraction by Rho-GDI monitored by real-time fluorescence resonance energy transfer. *Biochemistry*. 38:1744–1750.
Ochs, H.D. 1998. The Wiskott-Aldrich Syndrome. *Semin. Hematol.* 35:332–345.
Pollard, T.D., and J.A. Cooper. 1984. Quantitative analysis of the effect of *Acanthamoeba* profilin on actin filament nucleation and elongation. *Biochemistry*. 23:6631–6641.
Prehoda, K.E., D.J. Lee, and W.A. Lim. 1999. Structure of the Enabled/VASP Homology 1 domain-peptide complex: a key component in the spatial control of actin assembly. *Cell*. 97:471–480.
Regazzi, R., A. Kikuchi, Y. Takai, and C.B. Wolheim. 1992. The small GTP-binding proteins in the cytosol of insulin-secreting cells are complexed to GDP dissociation inhibitor proteins. *J. Biol. Chem.* 267:17512–17519.
Rohatgi, R., L. Ma, H. Miki, M. Lopez, T. Kirchhausen, T. Takenawa, and M.W. Kirschner. 1999. The interaction between N-WASP and the Arp2/3 complex links Cdc42-dependent signals to actin assembly. *Cell*. 97:221–231.
Spudich, J.A., and S. Watt. 1971. The regulation of rabbit skeletal muscle contraction. I. Biochemical studies of the interaction of the tropomyosin-troponin complex with actin and the proteolytic fragments of myosin. *J. Biol. Chem.* 246:4866–4871.
Suetsugu, S., H. Miki, and T. Takenawa. 1999. Identification of two human WAVE/SCAR homologues as general actin regulatory molecules which associate with the Arp2/3 complex. *Biochem. Biophys. Res. Commun.* 260:296–302.
Svitkina, T.M., and G.G. Borisy. 1999. Arp2/3 complex and actin depolymerizing factor/cofilin in dendritic organization and treadmilling of actin filament array in lamellipodia. *J. Cell Biol.* 145:1009–1026.
Taunton, J., B.A. Rowning, M.L. Coughlin, M. Wu, R.T. Moon, T.J. Mitchison, and C.A. Larabell. 2000. Actin-dependent propulsion of endosomes and lysosomes by recruitment of N-WASP. *J. Cell Biol.* 148:519–530.
Ting-Beall, H.P., Needham, D., and R.M. Hochmuth. 1993. Volume and osmotic properties of human neutrophils. *Blood*. 81:2774–2780.
Vinson, V.K., E.M. De La Cruz, H.N. Higgs, and T.D. Pollard. 1998. Interactions of *Acanthamoeba* profilin with actin and nucleotides bound to actin. *Biochemistry*. 37:10871–10880.
Weiner, O.D., G. Servant, M.D. Welch, T.J. Mitchison, J.W. Sedat, and H.R. Bourne. 1999. Spatial control of actin polymerization during neutrophil chemotaxis. *Nat. Cell Biol.* 1:75–81.
Welch, M.D., A.H. DePace, S. Verma, A. Iwamatsu, and T.J. Mitchison. 1997a. The human Arp2/3 complex is composed of evolutionarily conserved subunits and is localized to cellular regions of dynamic actin filament assembly. *J. Cell Biol.* 138:375–384.
Welch, M.D., A. Iwamatsu, and T.J. Mitchison. 1997b. Actin polymerization is induced by Arp2/3 protein complex at the surface of *Listeria monocytogenes*. *Nature*. 385:265–269.
Welch, M.D., J. Rosenblatt, J. Skoble, D.A. Portnoy, and T.J. Mitchison. 1998. Interaction of human Arp2/3 complex and the *Listeria monocytogenes* ActA protein in actin filament nucleation. *Science*. 281:105–108.
Winter, D., T. Lechler, and R. Li. 1999a. Activation of the yeast Arp2/3 complex by Bee1p, a WASP-family protein. *Curr. Biol.* 9:501–504.
Winter, D.C., E.Y. Choe, and R. Li. 1999b. Genetic dissection of the budding yeast Arp2/3 complex: a comparison of the in vivo and structural roles of individual subunits. *Proc. Natl. Acad. Sci. USA*. 96:7288–7293.
Yarar, D., W. To, A. Abo, and M.D. Welch. 1999. The Wiskott-Aldrich syndrome protein directs actin-based motility by stimulating actin nucleation with the Arp2/3 complex. *Curr. Biol.* 9:555–558.
Zhu, Q., C. Watanabe, T. Liu, D. Hollenbaugh, R.M. Blaese, S.B. Kanner, A. Aruffo, and H.D. Ochs. 1996. Wiskott-Aldrich syndrome/X-linked thrombocytopenia: WASp gene mutations, protein expression, and phenotype. *Blood*. 90:2680–2689.
Zigmond, S.H., M. Joyce, J. Borleis, G.M. Bokoch, and P.N. Devreotes. 1997. Regulation of actin polymerization in cell-free systems by GTPγS and Cdc42. *J. Cell Biol.* 138:363–374.